DOI: 10.1002/chem.200401352

Gas-Phase Dehydrogenation of Methanol with Mononuclear Vanadium-Oxide Cations

Marianne Engeser,[a, b] Detlef Schröder,*[a] and Helmut Schwarz[a]

Abstract: The reactions of methanol with mass-selected V^+, VOH^+, VO^+, and VO_2^+ cations are studied by Fourier-transform ion-cyclotron resonance (FT-ICR) mass spectrometry in order to investigate the influence of the formal oxidation state of the metal on the reactivity of vanadium–oxide compounds. Interestingly, the most reactive species is the low-valent hydroxide cation VOH^+, for which a formal condensation reaction prevails to afford $VOCH_3^+$. In contrast, atomic V^+ is oxidized and the high-valent dioxide cation VO_2^+ is reduced by methanol. The dehydrogenation of methanol mediated by VO^+ does not involve any change of the metal's oxidation state. For the latter reaction, the experimental results are complemented by a theoretical investigation by using density functional theory.

Keywords: mass spectrometry · metal alkoxides · methanol · oxidation · vanadium

Introduction

Transition-metal oxides play a tremendous role in heterogeneous catalysis. One major application is their use in oxidation reactions. Two important examples of oxidation catalysis using vanadium oxides are the oxidation of SO_2 to SO_3 for the production of sulfuric acid and that of butane to afford maleic anhydride.[1–23] It has been proposed that the alkane oxidation by transition-metal-oxide catalysts proceeds via alcohols and alkoxides as intermediates.[1,2,4] Furthermore, methanol oxidation itself yields valuable products such as formaldehyde and formic acid.[1,5] Like in many complicated heterogeneously catalyzed oxidation reactions, there are still a lot of mechanistic puzzles to be solved—also in vanadium-oxide-mediated catalysis.[1a,6] In particular, the roles of formal oxidation states and functional groups that form the "active sites" of a catalyst are of interest. In that respect, some fundamental insight might be gained by studying the reactivity of small model systems.[7] In the extreme case, these may be isolated molecules—if not atoms—in the gas phase.[8,9] By this approach, the reaction conditions can be controlled very accurately, and obscuring effects such as surface defects, aggregation phenomena, fast subsequent reactions, solvent and others are avoided. This reductionistic approach, down to the most simple model system, facilitates an understanding of the role of electronic structures on mechanistic details at a molecular level, but also entails that a direct extrapolation of the findings to applied catalysis may well be impossible.[10]

The present work describes the ion–molecule reactions of the mass-selected vanadium cations V^+, VO^+, VOH^+, and VO_2^+ with methanol. The aim is to investigate the influence of the metal's formal oxidation state and the reactivity of isolated functional groups (i.e., V=O, V–OH). The experimental results are complemented by some theoretical work on the VO^+-mediated dehydrogenation of methanol to clarify the roles of the oxo ligand and the metal. Our investigation is part of collaborative experimental and theoretical efforts in the Berlin area[11] on the mechanisms of oxidation reactions catalyzed by transition-metal oxides with a particular focus on the industrially important vanadium oxide catalysts. In addition, this investigation constitutes an extension of our previous work on the ion chemistry of vanadium alkoxides[12–14] and the mechanisms of alkane oxidation by vanadium oxides.[15,16] Recently, the reactions of methanol with mass-selected V^+ and VO^+ have been investigated by Cao et al. using ion-cyclotron-resonance (ICR) mass spectrometry as well as theoretical methods.[17] Moreover, Castleman and co-workers described the reactions of methanol with $M_xO_y^+$ clusters (M = V, Nb) and included the mononuclear

---

[a] Dr. M. Engeser, Dr. D. Schröder, Prof. Dr. H. Schwarz
Institut für Chemie der Technischen Universität Berlin
Strasse des 17. Juni 135, 10623 Berlin (Germany)
Fax: (+49) 30-314-21102
E-mail: detlef.schroeder@tu-berlin.de

[b] Dr. M. Engeser
Present address:
Kekulé-Institut für Organische Chemie und Biochemie
der Universität Bonn
Gerhard-Domagk-Strasse 1, 53121 Bonn (Germany)

ions VO^+ and VO_2^+ for comparison.[18] These results will be discussed in the context of our findings described herein.

Methods

Ion–molecule reactions were examined with a Spectrospin CMS 47X FTICR mass spectrometer equipped with an external ion source as described elsewhere.[19,20] In brief, V^+ was generated by laser ablation of a vanadium target by using a Nd/YAG laser operating at 1064 nm. A series of potentials and ion lenses was used to transfer the ions to the ICR cell, which was positioned in the bore of a 7.05 T superconducting magnet. Mass-selected $^{51}V^+$ was then subjected to a pulse of argon or converted to VO^+ by reaction with pulsed-in O_2, respectively.[21] VO_2^+ was prepared by using a pulse of N_2O.[15] During the gas pulses, the ions undergo several hundreds of collisions so that the product ions were assumed to be thermalized.[22] The reactivity of the subsequently mass-selected ion of interest was studied by introducing methanol by a leak valve at stationary pressures in the order of 10^{-8} mbar. The experimental second-order rate constants were evaluated assuming the pseudo first-order kinetic approximation after calibration of the measured pressures and acknowledgement of the ion gauge sensitivities.[23] The error of the absolute rate constants is ±30%, while the error for the relative rate constants amounts to only 10%. To study the reactivity of VOH^+, the product ion VOH^+ formed in the reaction of V^+ with methanol was thermalized with another pulse of argon and mass-selected before its reactivity was monitored as described above.

All calculations employed the hybrid density functional theory (DFT) B3LYP method[24] as implemented in the Gaussian 98 program package.[25] After a preliminary scan of the potential-energy surfaces with the Lanl2DZ basis sets,[26] the relevant structures were re-optimized with the Ahlrichs valence triple-ζ basis sets with polarization functions on all atoms,[27] which was used in a previous benchmark study for vanadium alkoxides.[12] For all stationary points obtained, vibrational frequencies were computed at the same level of theory in order to confirm that these correspond to local minima (no imaginary frequency) or transition structures (one imaginary frequency) or higher-order saddle points. All energies given below refer to 0 K and include zero-point energy (ZPE).

Results and Discussion

This section is organized as follows: A description and discussion of the primary ion–molecule reactions of the four selected cations, in conjunction with a comparison to previous measurements,[17,18] is followed by a presentation of theoretical results of one of these reactions, that is, the dehydrogenation of methanol by VO^+. The subsequent reactions of the products formed in the primary ion–molecule reactions are then described. The section closes with a discussion of the results in the context of previous studies on vanadium alkoxides,[12] and the reactivity of other transition-metal oxides in the gas phase.[28,29,30]

Primary ion–molecule reactions: Four different cationic vanadium species have been selected for this work. The two plain vanadium oxides VO^+ and VO_2^+ cover the oxidation states +III and +V, respectively. For comparison, the hydroxide VOH^+ (+II) and atomic V^+ (+I) ions were also studied. The measured rate constants, reaction efficiencies and primary branching ratios for the reactions with methanol are summarized in Table 1. For all cases, except VOH^+, reaction efficiencies in the order of only $\phi = 10\%$ are observed, which indicate thermochemical restrictions for product formation and/or the existence of substantial kinetic barriers; here, the reaction efficiency is defined as $\varphi = k_R/k_C$ where k_R is the experimentally measured rate constant and k_C corresponds to the gas-kinetic collision rate.[31]

Table 1. Experimental second-order rate constants (k), reaction efficiencies (ϕ)[a] and primary neutral products[b] for the ion–molecule reactions of methanol with cationic vanadium species in different oxidation states.

Ion Oxidation state	V^+ I	VOH^+ II	VO^+ III	VO_2^+ V
k[c]	2.5	14.0	1.2	2.0
ϕ	10	70	6	10
$-H_2$			95	
$-H_2O$		>90		28
$-CH_2O$				72
$-CH_4$	70	<5	5	
$-CH_3$	30	<5		

[a] Efficiency relative to the gas-kinetic collision rate calculated according to ref. [31c]. [b] Intensities are normalized to a sum of 100%. [c] Given in $10^{-10}\,cm^3\,molecule^{-1}\,s^{-1}$. The error is assumed to be ±30%.

The reaction of V^+ with methanol is dominated by the formation of VO^+ concomitant with the liberation of methane. The abstraction of the oxygen atom from methanol is strongly exothermic ($\Delta_rH = -204\,kJ\,mol^{-1}$, Table 2). As a minor channel, the loss of a methyl radical by OH abstraction is observed as well ($\Delta_rH = -46\,kJ\,mol^{-1}$) and provides access to the VOH^+ cation for further reactivity studies. These results qualitatively agree with the experimental data of Cao et al.[17] who, however, did not report branching ratios. The abundance of VOH^+ exceeds that of VO^+ in their experiments, which might be explained by the omission of an efficient thermalization step prior to the reactivity studies, of which we took particular care.[21]

Table 2. Heats of formation [$kJ\,mol^{-1}$][a] of species used in the data analysis.

	Δ_fH		Δ_fH
V^+	1162 ± 8[b]	$CH_3^{\bullet}$	146.5 ± 0.5[f]
VO^+	832 ± 12[c]	CH_4	−74.9 ± 0.3[g]
VOH^+	768 ± 15[d]	CH_2O	−108.6 ± 0.5[b]
VO_2^+	716 ± 16[e]	$CH_3O^{\bullet}$	17 ± 4[f]
O	249.2 ± 0.1[b]	CH_3OH	−201.1 ± 0.2[g]
OH	39.3 ± 0.2[f]	H_2O	−241.8 ± 0.1[g]

[a] Values for gaseous species at 298 K. [b] Ref. [68]. [c] Derived using $D_0(V^+{-}O) = 5.99 \pm 0.1$ eV (ref. [66]). [d] Derived using $D_0(V^+{-}OH) = 4.50 \pm 0.15$ eV (ref. [66]). [e] This work, see text. [f] Ref. [69]. [g] Ref. [59].

Oxygen atom and OH abstraction are also observed when VOH^+ interacts with methanol, but only in very low levels. A new channel, the formation of $[VCH_3O]^+$, dominates the product pattern by far. Formally, this pathway corresponds to a condensation reaction forming $VOCH_3^+$ and a neutral water molecule and can hence be regarded as a replacement of the hydroxy ligand in VOH^+ by a methoxy group. The enhanced reaction rate, compared with the atomic or higher oxide cations of vanadium, can be ascribed to the presence of the hydroxyl group, which opens up a new and strongly favored reaction channel during which no redox reaction is involved. No thermochemical data for the product ion $VOCH_3^+$ is available in the literature so far. Its formation from VOH^+ and methanol in an ICR experiment implies $\Delta_fH(VOCH_3^+) \leq 809 \pm 20$ kJ mol^{-1} and thus a lower limit of $D(V^+{-}OCH_3) = 370 \pm 25$ kJ mol^{-1}.[32,33] Given the absence of $V(OCH_3)^+$ as a product in the reaction of V^+ with CH_3OH, we may furthermore cautiously propose an upper limit of $D(V^+{-}OCH_3) < D(H{-}OCH_3) = 435 \pm 4$ kJ mol^{-1}. The free reaction enthalpy of the reaction $^4VOH^+ + CH_3OH \rightarrow {}^4VOCH_3^+ + H_2O$, calculated at the same B3LYP-TZVP level as used in the computational studies described below, amounts to $\Delta G_{298} = -41$ kJ mol^{-1}.[34] A slight exothermicity of the OH/OCH_3 exchange is consistent with the occurrence of this reaction under ICR conditions as well as previous findings for the analogous ions of iron.[35] Accordingly, for a thermochemical estimate we combine the experimental data of VOH^+, CH_3OH, and H_2O with the computed exothermicity, which leads to a bond energy in the range of $D(V^+{-}OCH_3) = 410 \pm 40$ kJ mol^{-1}. A comparison of the bond strengths in $VOCH_3^+$ and VOH^+ reveals strong similarities; this suggests that the V–O bond is not largely affected by the $VOH^+ \rightarrow VOCH_3^+$ conversion. Interestingly, however, $D(V^+{-}OCH_3) = 410 \pm 40$ kJ mol^{-1} implies that $D(VO^+{-}CH_3) = 210 \pm 20$ kJ mol^{-1} and thus points to an unusually weak C–O bond in $VOCH_3^+$ compared with the typical C–O bond strengths, for example, $D(H_3C{-}OH) = 387 \pm 1$ kJ mol^{-1} (Table 2).

The main pathway (95%) in the reaction of VO^+ with methanol gives rise to the elimination of molecular hydrogen. The intuitive assignment of the product ion $[VCH_2O_2]^+$ as the formaldehyde complex $OV(OCH_2)^+$, formed by a selective 1,2-dehydrogenation, is corroborated by the exclusive loss of HD when reacting CD_3OH with VO^+. D_2 loss, corresponding to a 1,1-elimination, is not observed. Furthermore, the presence of a formaldehyde unit in $[VCH_2O_2]^+$ is indicated by the rapid consecutive reaction of this ion with methanol to afford $[VCH_4O_2]^+$, which implies an exchange of a CH_2O ligand by CH_3OH (see below). Given the formation of $OV(OCH_2)^+$, the dehydrogenation of methanol by VO^+ therefore is not associated with a change in the oxidation state of the metal. Somewhat intriguing is the finding that VO_2^+ is also formed from methanol/VO^+ in low, but reproducible yields of about 5%, since methane formation indicates $D(OV^+{-}O) \geq \Delta_fH(CH_3OH)\text{-}\Delta_fH(O)\text{-}\Delta_fH(CH_4) = 375 \pm 20$ kJ mol^{-1}, where the margin of error acknowledges the uncertainty associated with thermal contributions in the measurements conducted at 298 K.[32] This value is higher than the one reported from guided-ion-beam (GIB) experiments of $D_0(OV^+{-}O) = 295 \pm 39$ kJ mol^{-1}.[36] Even though the GIB technique usually provides reliable thermochemical data, this particular value might have been underestimated, because it was derived from the apparent threshold of the very endothermic reaction $VO^+ + CO \rightarrow VO_2^+ + C$ that has to compete with the less endothermic and therefore favored formation of $V^+ + CO_2$. In fact, more recent collision-induced dissociation experiments yield $D_0(OV^+{-}O) = 339 \pm 35$ kJ mol^{-1},[37] which is in good agreement with the broader range of $D_0(OV^+{-}O) = 333 \pm 43$ kJ mol^{-1} obtained by ICR bracketing.[15] Furthermore, theoretical values such as $D_0(OV^+{-}O) = 377$ kJ mol^{-1} and 423 kJ mol^{-1} have been reported.[15,38] As indicated by the formation of VO_2^+ by reduction of methanol to methane, the bond-dissociation energy should lie closer to the upper end of the reported experimental error bars. In combining the values $D_0(OV^+{-}O) = 339 \pm 35$ kJ mol^{-1}, $D_0(OV^+{-}O) = 333 \pm 43$ kJ mol^{-1}, and $D(OV^+{-}O) \geq 375 \pm 20$ kJ mol^{-1}, we arrive at $D(OV^+{-}O) = 365 \pm 10$ kJ mol^{-1} and hence $\Delta_fH(VO_2^+) = 716 \pm 16$ kJ mol^{-1}, which is used in the following. The efficiency of the reaction of methanol with VO^+ ($\phi = 6\%$) is even lower than for V^+ and VO_2^+ (Table 1). As both the reactants and the products exhibit triplet ground states (see below), a kinetic barrier caused by a transition structure located energetically close to the entrance channel may provide an explanation for the low reaction efficiency. Alternatively, a spin-induced kinetic bottleneck in terms of two-state reactivity[39] is also conceivable. While our experimental findings in the VO^+/CH_3OH system are consistent with the qualitative studies of Cao et al.,[17] some disagreement evolves in comparison with the work of Justes et al.[18]. They reported the formation of $VOCH_3^+$, which could neither be observed in the ICR experiments of Cao et al., nor in the present ICR study, nor in independent experiments obtained using a multipole instrument.[14] In addition, the estimate $D(VO^+{-}CH_3) = 210 \pm 20$ kJ mol^{-1} derived above contradicts an exothermic methyl transfer from methanol to VO^+ as $D(CH_3{-}OH) = 386 \pm 1$ kJ mol^{-1}. Among others, a possible rationale is that the mode of mass selection of VO^+ in the experiments described by Justes et al.[18] was not perfect in that some VOH^+ was present in the mass-selected beam. In view of the fact that the reaction of VOH^+ with methanol is an order of magnitude faster than that of VO^+ (Table 1), significant amounts of $VOCH_3^+$ could in fact be expected in this case. Furthermore, both previous studies mention the generation of the formal adduct complex $[VCH_4O_2]^+$ as an ionic product.[17,18] We also observe $[VCH_4O_2]^+$ in the ICR experiments described here, but can clearly attribute it to a secondary reaction of initially formed $OV(OCH_2)^+$ with methanol (see below). It is possible, however, that the differences reported with respect to $[VCH_4O_2]^+$ are associated with the different pressure regimes of the experiments. The ICR studies conducted at extremely low pressure (typically, 10^{-8} mbar) disfavor association reactions, whereas termolecular stabilization may play a significant role in the experiments of Justes et al., which were conducted at significantly higher pressures (typically, 10^{-4} mbar).[18]

The reaction of methanol with VO_2^+, the oxide in the highest oxidation state possible for a vanadium compound, is associated with the reduction to V^{III} in all reaction channels observed. These include the loss of water to yield the same ionic product $OV(OCH_2)^+$ as in the methanol/VO^+ case. In addition to the expulsion of H_2O, a formaldehyde molecule can be released. The latter route is approximately three times more favored than the expulsion of H_2O. The preference for the second reaction pathway may be ascribed to the formation of relatively stable $VO_2H_2^+$ species for which two isomers are conceivable, that is, the water complex $OV(OH_2)^+$ and the thermochemically more stable dihydroxide cation $V(OH)_2^+$.[21,40] Similar to the findings reported earlier for a related system, both isomers are expected to be accessible, as the energies needed for the second hydrogen shift either to the OH or to the O ligand should be comparable. Thus, the energetic difference of the barrier height (ΔE) associated with hydrogen shift from $OV(OCH_3)_3^+$ to form $HOV(OCH_3)_2(OCH_2)^+$ ($\Delta E = 0.82$ eV) and the one to produce $OV(OCH_3)(OCH_2)(CH_3OH)^+$ ($\Delta E = 0.83$ eV) is only marginal according to DFT calculations with a TZVP basis set.[12] Irrespective of the actual isomer formed initially, the reaction is very exothermic allowing for a subsequent isomerization from $VO(OH)_2^+$ to $VO(H_2O)^+$; in addition, a second methanol molecule might catalyze the transformation by a proton-shuttle mechanism.[21,40,41] Finally, VO^+ is found in the methanol/VO_2^+ experiment in traces of maximum 1%. Even though it is therefore difficult to decide with certainty whether this is really a primary product, its formation by loss of both ligands from the postulated intermediate $OV(OCH_2)(H_2O)^+$ is feasible and thermochemically possible ($\Delta_rH = -33\,\text{kJ mol}^{-1}$). There is again some deviation compared with the data of Justes et al.[18] They observe the $VO_2H_2^+$ product as well, but also report the formation of $VO_2CH_3^+$, whereas we observe $OV(OCH_2)^+$ under ICR conditions. The present results agree with the formation of $VO_2C_2H_6O^+$ (m/z 129) reported by Justes et al., which can be ascribed to a consecutive reaction of the $OV(OCH_2)^+$ product with neutral methanol (see below).

In conclusion, the oxidation state of the metal and the oxophilicity of vanadium dictate the reactivity of the corresponding cation. In the case of atomic V^+ (V^I), the oxygen atom is transferred to the metal and methanol is reduced to methane or methyl. A reduction of methanol is also possible with the V^{II} species VOH^+, but cannot compete efficiently with the formation of $V(OCH_3)^+$, because the hydroxyl group allows for a formal ligand substitution reaction without involvement of redox processes. The monoxide cation VO^+ (V^{III}) mediates dehydrogenation of methanol to formaldehyde without changing the oxidation state of the metal. In contrast, the reaction of VO_2^+ (V^V) with methanol also leads to formaldehyde, either as a ligand or as a free molecule, but here the metal is reduced to V^{III}. The reaction can therefore be classified as an oxidative dehydrogenation.

Even though V^+ does not dehydrogenate methanol, it is able to dehydrogenate nonactivated alkanes.[42] In fact, the product patterns in the reactions of V^+ and VO^+ with hydrocarbons are very much alike, except that VO^+ is much less reactive.[42] The pronounced difference of the reactivities of the two ions towards methanol reported here can be ascribed to the strong oxophilicity of the early transition metal vanadium. Thus, the abstraction of an oxygen atom from oxygen-containing compounds such as methanol is favored, similar to what has already been reported for butanone.[43] However, the presence of an oxo ligand reduces the oxophilicity in that VO^+ only forms methane from methanol in very small amounts. Instead, another reaction channel (dehydrogenation) is strongly favored. The second oxygen ligand in VO_2^+ finally makes the cation a stronger oxidant, not promoting simple dehydrogenation (as does VO^+), but rather oxidative dehydrogenation. All of these observations are very much in accordance with the oxidation state V^{III} being more stable than V^I, V^{II} and V^V, as expected in analogy to solution-phase chemistry.[44]

Computational aspects—Mechanism of methanol dehydrogenation by VO^+: It has often been demonstrated in recent years that applied computational chemistry is essential for the fruitful interplay of experiment and theory in gas-phase chemistry.[45–47] Improvements in density functional theory, particularly hybrid methods, have very much extended the scope of theoretical studies as far as size and complexity are concerned.[48] Nowadays, even reactions of transition-metal compounds can be studied theoretically with reasonable accuracy and reliability. Nevertheless, computational studies of coordinatively unsaturated transition-metal complexes still remain quite demanding, both in terms of computing resources as well as intellectual input. Hence, instead of an exhaustive theoretical investigation of all reactions described here, we decided for a more selective approach. Specifically, the dehydrogenation of methanol by VO^+ was chosen on the following grounds.

The reaction of $VO^+ + CH_4 \rightarrow V^+ + CH_3OH$ had been studied previously,[49] and the results are fully consistent with the present experimental findings as well as those of Cao et al.[17] and their theoretical work. Furthermore, the reaction of VOH^+ with methanol is dominated by a formal OH/OCH_3 exchange, a condensation process which is considered of remote interest in the context of oxidation catalysis. The product pattern for $VO_2^+ + CH_3OH$ suggests an oxidative dehydrogenation of methanol. While this process is of interest, previous theoretical investigations of the reactions of VO_2^+ with ethene,[15,50] ethane,[15,40] and propane[16] are considered to have provided a general insight into the mechanisms of oxidative dehydrogenation by VO_2^+ in the gas phase. In distinct contrast, the VO^+-mediated dehydrogenation of methanol poses several questions concerning the details of the reaction mechanism. Although the experimental results for the dehydrogenation of methanol by VO^+ clearly prove the operation of a 1,2-elimination to produce formaldehyde, it is feasible for several structural types of intermediates to play a role in this process, that is, alkoxides, metal hydrides, carbenes and others. Density functional theory is used as a theoretical tool to further investigate this reaction, because it allows satisfactory results with reasonable costs in many cases.[51] Yet, verification by ab initio studies is necessary. The results obtained so far for related systems do not contradict the suitability of DFT to describe the reactivity of small vanadium oxides with sufficient accuracy.[12,14,52,53] For the problem studied here, one has to consider another point though. For similar systems, it has been shown that the reaction of a cationic metal oxide with alcohols can proceed through OH abstraction and formation of charge-transfer complexes.[29] While such two-component intermediates, with methanol as a model substrate, are surely difficult to describe by quantum-chemical methods, these problems should not play a role here, since these mechanisms are expected to dominate in bigger systems only, in which carbocations significantly more stable than CH_3^+ might form.

Three scenarios are conceivable for the chemical activation of methanol: i) breakage of the O–H bond, ii) activation of a C–H bond, and iii) cleavage of the C–O bond.[54] In all three cases, the new bond in a reaction with diatomic MO^+ (Scheme 1, M = V) can be formed a) to the metal or b) to the oxygen atom. Cases i-b) and iii-b) both result in the formation of the intermediate CH_3OMOH^+. For all hypothetical intermediates depicted in Scheme 1, their further reactions leading to $OM(OCH_2)^+$ are easily conceivable; maybe with the exception of iii-a). Experimental results for the reaction of FeO^+ with methanol were interpreted in terms of a direct activation of the O–H bond leading to CH_3OFeOH^+, which can be attributed to mechanism i-b).[29] In contrast, it was postulated for MoO^+ that CH_2O formation from methanol is initiated by C–H bond activation and proceeds via a molybdenum hydride species (case ii-a).[30] For molybdenum, the insertion in the C–O bond is only observed with larger alcohols and leads to dehydration. In this scenario, molybdenum–alkyl intermediates are assumed to play a major role (case iii-a). For the specific reaction discussed here, route iii) is not considered in detail, because a reaction leading to $OV(OCH_2)^+$, after breaking the C–O bond, has to return to one of the intermediates discussed for pathways i) and ii).[55]

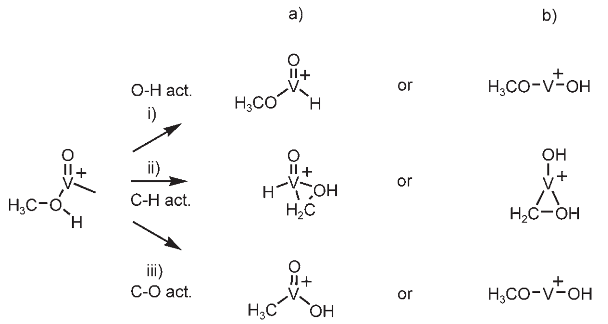

Scheme 1. Mechanistic scenarios for the initial bond-activation steps in the dehydrogenation of methanol by VO^+.

In the following, the main stationary points found on the B3LYP/TZVP level for the conceivable reactions of methanol with VO^+ are presented according to the classification given in Scheme 1. As the reactant VO^+ possesses a triplet ground state, both the triplet and singlet potential-energy surfaces have been considered.

The reaction of VO^+ with methanol commences with the formation of adduct complex **1** (Figure 1) with geometric features similar to the separated reactants, except that the C–O bond is slightly elongated to 148 pm compared with 142 pm in free methanol (Figure 2). For the activation of the O–H bond, a triplet transition structure **TS1/3** has been found 34 kJ mol^{-1} below the entrance channel $VO^+ + CH_3OH$. It connects the adduct complex $VO(CH_3OH)^+$ (**1**) directly with the inserted species CH_3OVOH^+ (**3**); similar energetics were reported in reference [17]. In **TS1/3**, the atoms OVOH form a nearly planar four-membered ring. The distance from the metal to the transferred hydrogen atom (d(V–H) = 193 pm) is significantly longer than in the hydride structure **2** located on the singlet surface only (d(V–H) = 155 pm, Figure 2). A transition structure corresponding to **TS1/3** was also found on the singlet surface; but with 67 kJ mol^{-1} above the entrance channel it is much too high in energy to play a role in a gas-phase experiment conducted at thermal energy. In contrast, the (singlet) transition structures **TS1/2** and **TS2/3** for two subsequent 1,2-hydrogen transfers are situated energetically close to the entrance channel (+22 kJ mol^{-1} and −1 kJ mol^{-1}, respectively). Therefore, the inserted species **3** might also be reached

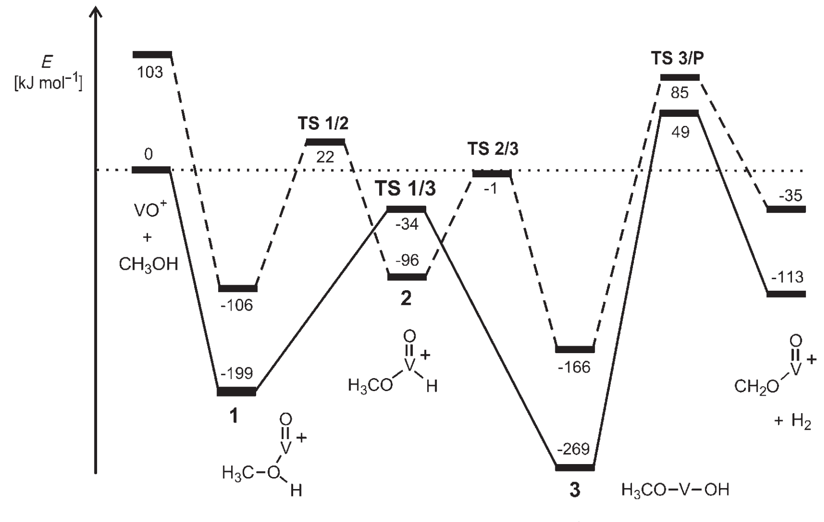

Figure 1. Energy diagram for the dehydrogenation of methanol with VO^+ initiated by activation of the O–H bond, calculated at the B3LYP/TZVP level. Energies include ZPE and are given in kJ mol^{-1} relative to the entrance channel $^3VO^+ + CH_3OH$ (E_{abs} = 1018.964283 + (−115.719947) = −1134.68423 Hartree). Solid line: triplet surface; dashed line: singlet surface.

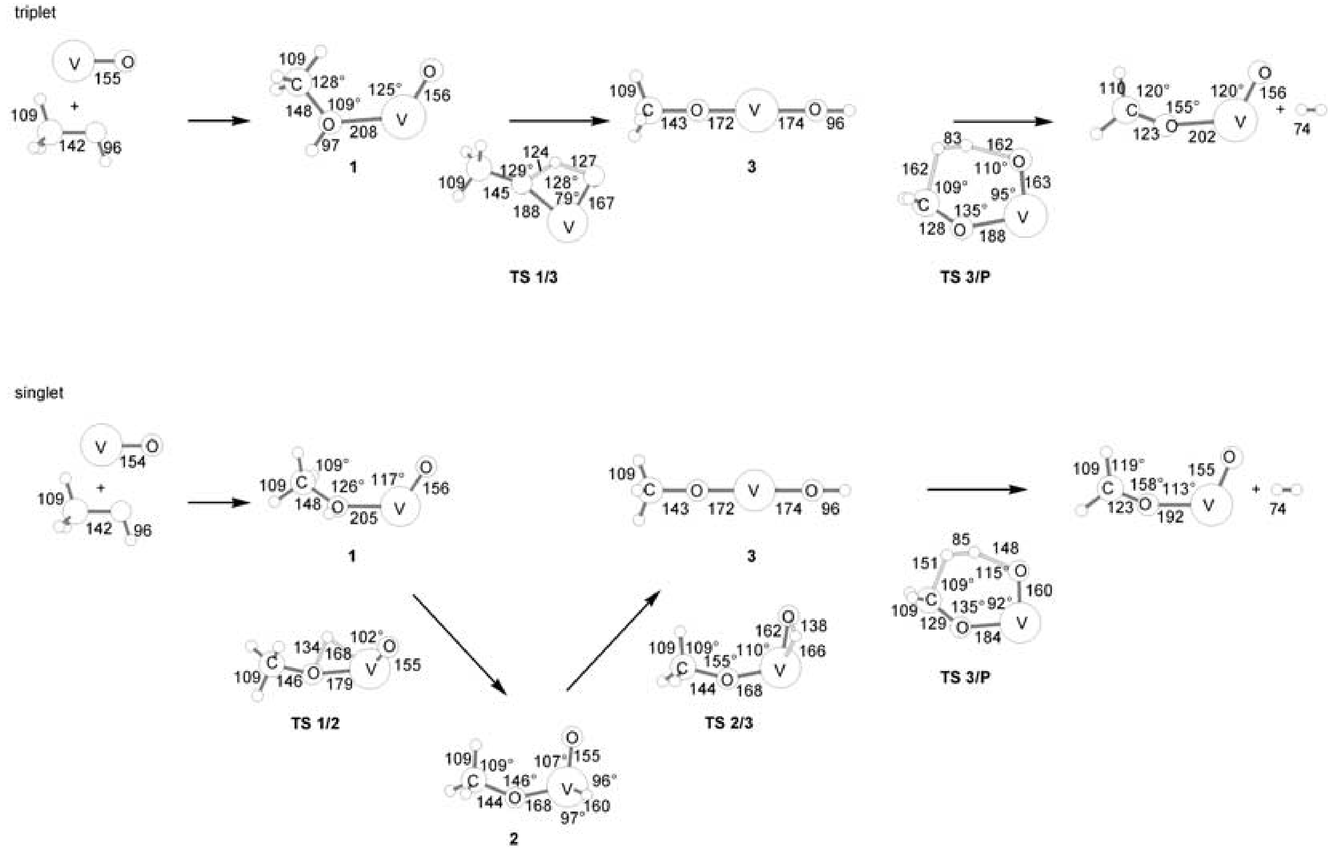

Figure 2. Relevant geometric data for the species involved in the reaction pathways shown in Figure 1; bond lengths are given in pm.

through a double spin-state change, provided the spin inversion is sufficiently effective and the crossing points are appropriately positioned.[39b] The latter pathway, with participation of the singlet intermediate **2**, could be classified as case i-a), whereas the direct formation of **3** via **TS1/3** corresponds to case i-b).

As expected, the linear product CH_3OVOH^+ (**3**) forms the global minimum of the potential-energy surface ($-269\,kJ\,mol^{-1}$). Starting from **3**, the exit channel $(CH_2O)VO^+ + H_2$ may be reached directly via **TS3/P**. This route does not include a complex $(CH_2O)VO^+{\cdot}(H_2)$ with a coordinated hydrogen molecule.[56] However, as its barrier lies $49\,kJ\,mol^{-1}$ above the entrance channel, this pathway cannot play a role in the ICR experiments described above. During the pre-optimization on the B3LYP/Lanl2DZ level, some other transition structures have been found which connect the metal hydride **2** to the complex **6** (see below) or the exit channel. Nevertheless, all these saddle points are so high in energy that they were not considered any further ($+125\,kJ\,mol^{-1}$ above the separated reactants for the singlet and $+100\,kJ\,mol^{-1}$ for the triplet surface). Although it cannot be excluded with certainty that an energetically accessible transition structure leading from **3** to the exit channel or a complex $(CH_2O)VO^+{\cdot}(H_2)$ has escaped our intensive search, we conclude that a reaction pathway commencing with O–H bond activation (case i) is not involved in the VO^+-mediated dehydrogenation of methanol.

The initial activation of a C–H bond in the adduct complex **1** (case ii in Scheme 1) can proceed via **TS1/4** which is still energetically accessible (Figure 3). It represents a hydrogen-atom transfer from the carbon atom to the vanadyl oxygen atom in a single step. The V–H bond length is relatively short (d(V–H) = 172 pm) in **TS1/4**, which indicates a metal–hydrogen interaction, even though there are no V–H bonds in either **1** or **4** (Figure 4). Note that the structure of product **4** does not correspond to a VOH complex of protonated formaldehyde, but rather to a three-membered oxometallacycle with largely equivalent V–O and V–C bonds (Mulliken charge analysis: $q(VOH) = +0.85$, $q(HOCH_2) = +0.15$). The second step in methanol dehydrogenation, according to this route, consists of a hydrogen migration from the hydroxyl group of the former methanol moiety to the metal (**TS4/5**), which results in the intermediate $(CH_2O)V(OH)(H)^+$ (**5**). As **TS4/5** lies energetically close to the entrance channel, the entire internal energy of the system is needed for this step.[57] The last hydrogen transfer via **TS 5/6** is less energy demanding ($-52\,kJ\,mol^{-1}$) and forms the hydrogen complex **6** which easily dissociates to the products $(CH_2O)VO^+ + H_2$. Hence, the whole reaction can proceed on the triplet surface after initial C–H bond activation (case ii). The singlet potential-energy surface is situated about $90\,kJ\,mol^{-1}$ higher in energy and does not cross the triplet surface. The overall reaction pathway described here can be classified to case ii-b) in Scheme 1. The involvement of an

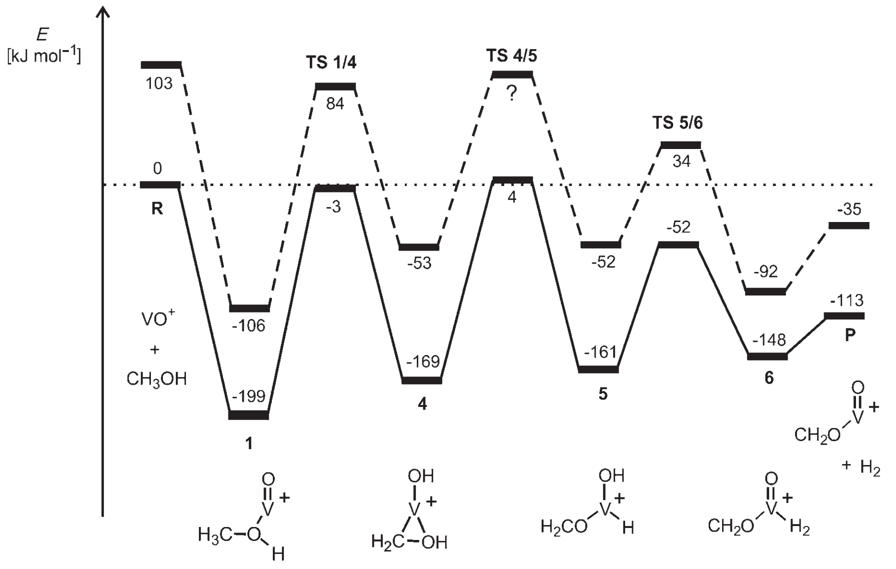

Figure 3. Energy diagram for the dehydrogenation of methanol with VO$^+$ initiated by activation of a C–H bond, calculated at the B3LYP/TZVP level. Energies include ZPE and are given in kJ mol^{-1} relative to the entrance channel $^3VO^+$ + CH_3OH (E_{abs} = 1018.964283 + (−115.719947) = −1134.68423 Hartree). Solid line: triplet surface; dashed line: singlet surface.

intermediate $HV(O)(CH_2OH)^+$, expected according to route ii-a), could already be ruled out during the pre-optimization process, in which the corresponding minimum was found 52 kJ mol^{-1} above the entrance channel.

In comparison, the theoretical results are in good agreement with the experimental observations. The reaction is exothermic with a calculated reaction energy of $\Delta E = -113$ kJ mol^{-1}. It does not proceed via an initial O–H bond activation along path i), because the dehydrogenation of the readily accessible intermediate **3** is prevented by an insurmountable barrier (Figure 1). In contrast, dehydrogenation of methanol is possible through an initial C–H bond activation along path ii-b): all barriers can be overcome starting from the entrance channel (Figure 3). Furthermore, spin restrictions do not play a role here because the energetically lowest pathway only proceeds on the triplet potential-energy surface. First, the vanada–oxirane structure **4** is formed, then the hydrogen atom of the hydroxyl group is transferred to the metal, and finally neutral H_2 is eliminated. Passing the first two barriers needs all the energy of the system, in accordance with the small reaction efficiency observed in the experiment. Note that the mechanism reported here cannot be considered as an VO-induced rearrangement of a methanol cation,[58] because an electron transfer in the adduct $(CH_3OH)VO^+$ (**1**) from the methanol moiety to VO^+ does not occur to a notable extent (Mulliken charge analysis: $q(VO) = +0.83$, $q(CH_3OH) = +0.17$), which is in accordance with the ionization energies of the separated entities, IE(VO) = 7.24 eV versus IE(CH_3OH) = 10.84 eV.[59]

Subsequent reactions: In the system methanol/VO$^+$, the initially formed dehydrogenation product $(CH_2O)VO^+$ reacts with another methanol molecule to form $[VCH_4O_2]^+$. Tentatively, this product is assigned to the adduct complex

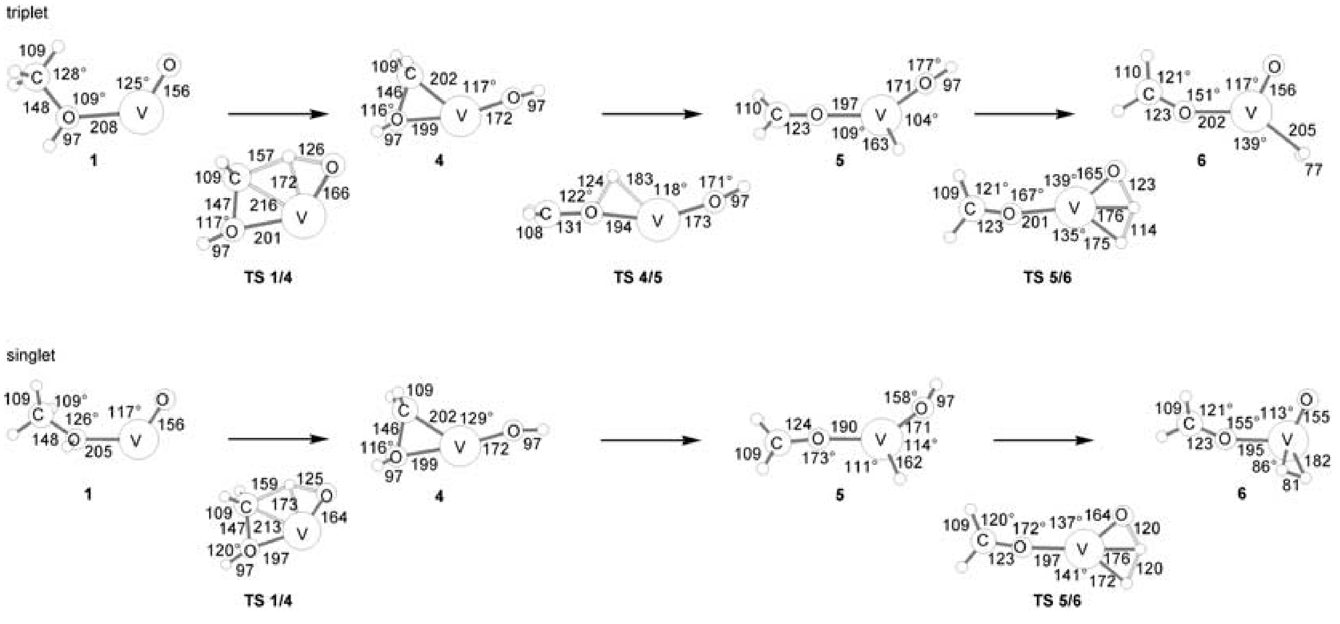

Figure 4. Relevant geometric data for the species involved in the reaction pathways shown in Figure 3; bond lengths are given in pm.

$(CH_3OH)VO^+$ (**1**), which can be formed by ligand exchange of formaldehyde against methanol. Other structures are feasible as well, that is, the insertion species CH_3OVOH^+ (**3**), as this isomer is more stable than the adduct **1**. The further reaction of $[VCH_4O_2]^+$ with methanol initiates a reaction cascade comprising a whole series of intermediates and branches, which all lead to $[VC_3H_{10}O_3]^+$ as the major final product (Figure 5). This observation is explained when considering the intermediate species $LVOH^+$ (L might be a methoxy group, for example) and subsequent condensation reactions in which the ions bearing a hydroxyl group react to yield vanadium alkoxides $LVOCH_3^+$ and neutral water. A good fit of the experimental data has been achieved for the reaction scheme shown in Scheme 2 in which the structure $V(OCH_3)_2(CH_3OH)^+$ is assigned to the final $[VC_3H_{10}O_3]^+$ product. Note that other models, including the mere coordination of methanol for example (grey arrows in Scheme 2),[60] allow an equally good approximation of the observed intensities, in particular due to the low intensity of the intermediates $[VC_2H_6O_3]^+$ (*m*/*z* 129) and $[VC_3H_8O_3]^+$ (*m*/*z* 143). Nevertheless, involvement of $LVOH^+$ ions as key intermediates in such a scenario contradicts the structure $(CH_3OH)VO^+$ assigned to the $[VCH_4O_2]^+$ product above. The barrier associated with the direct isomerization of $(CH_3OH)VO^+$ (**1**) to the more stable CH_3OVOH^+ (**3**) may even be lowered further by catalysis of another protic, polar molecule (i.e., water or methanol)[21,40] in analogy to the interconversion of the isomers $OV(OH_2)^+$ and $V(OH)_2^+$, which can be regarded as lower homologues of **1** and **3**.

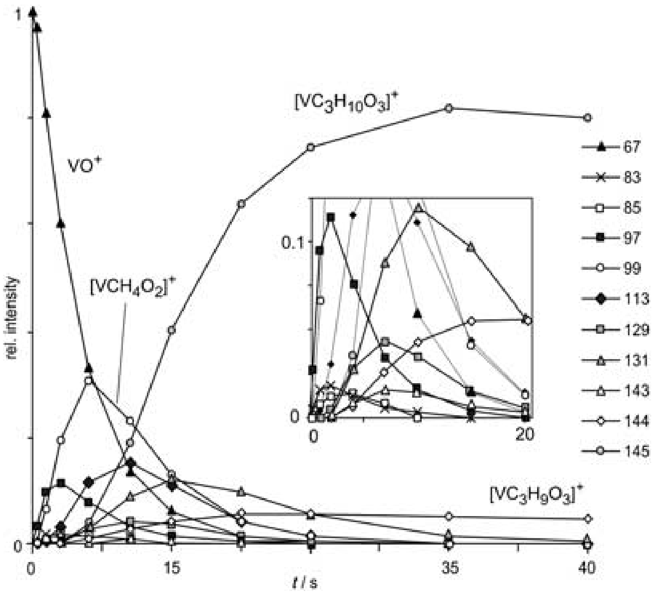

Figure 5. Intensities (normalized to $\Sigma = 100$) for the reaction of VO^+ with methanol at $p = 1.8 \cdot 10^{-8}$ mbar. Ions with intensities lower than 1% at all reaction times are not shown. The legend gives the masses of the observed ions (67: VO^+, 83: VO_2^+, 85: $VO_2H_2^+$, 97: $[VCH_2O_2]^+$, 99: $[VCH_4O_2]^+$, 113: $[VC_2H_6O_2]^+$, 129: $[VC_2H_6O_3]^+$, 131: $[VC_2H_8O_3]^+$, 143: $[VC_3H_8O_3]^+$, 144: $[VC_3H_9O_3]^+$, 145: $[VC_3H_{10}O_3]^+$). The inset shows a part of an enlarged view of the same diagram to clarify the progression of the less intense ions (*m*/*z* 83, 85, 143).

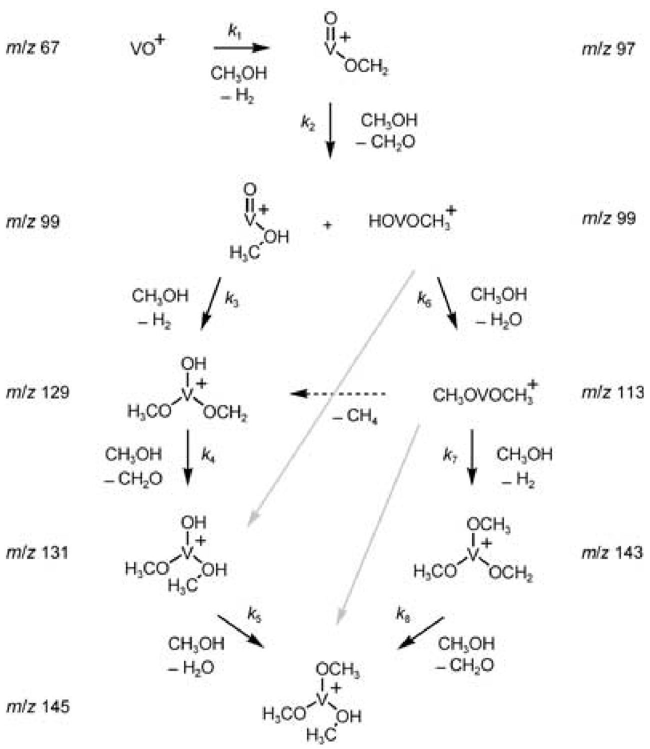

Scheme 2. Scheme of a reaction cascade leading from VO^+ to $V(OCH_3)_2(CH_3OH)^+$. A best fit of the experimental data shown in Figure 5 is obtained with the relative rate constants: $k_1 = 1$, $k_2 = 5.4$, $k_3 = 0.46$, $k_4 = 2.7$, $k_5 = 0.58$, $k_6 = 0.92$, $k_7 = 1.42$, $k_8 = 11.5$, $k_9 = 1.12$. Grey arrows: adduct formation, dashed arrow: methane elimination; for explanations and k_9 see text.

Interestingly, the reaction sequence of the methanol/VO^+ system begins and ends with a V^{III} species. Furthermore, all abundant intermediates can also be interpreted as formal V^{III} compounds (Scheme 2). In the major reaction pathways of the methanol/VO^+ system, a change in oxidation state is not involved throughout the whole sequence. Ligand exchange and condensation reactions obviously do not require a change of the oxidation state of the metal center. The dehydrogenation occurs in such a way that only the organic ligand is oxidized, but not the metal. Under the low-pressure conditions of the present ICR experiments, the reaction cascade ends with the probably sufficiently saturated coordination complex $V(OCH_3)_2(CH_3OH)^+$.

In a side reaction of the first step in the methanol/VO^+ system, formation of VO_2^+ occurs by methane elimination. The further reactions of this ion with methanol do not lead to other products than those already discussed, except for the ion $VO_2H_2^+$ (Table 1). Indeed, $VO_2H_2^+$ is observed during the methanol/VO^+ cascade in the expected small amounts (Figure 5, inset). Even though the side reaction of the very first step does not initiate significant pathways, it indicates the possibility of methane eliminations in the later steps of the reaction cascade to produce V^V species. For example, $V(OCH_3)_2^+$ (*m*/*z* 113) might react with methanol under loss of methane to afford the $VO(OCH_3)_2^+$ ion (m/z 129). An ion of this mass is indeed observed experimentally (Figure 5). Nevertheless, like in the first step, these oxidations may not compete effectively with the alternative eliminations of hydrogen and water. Therefore, formal V^V compounds are expected to account only for a very minor part of the product spectrum. In the example explicitly given above, the exact amount cannot be determined because $[VC_2H_6O_3]^+$ is also formed by another reaction channel (dashed arrow in Scheme 2). In conclusion, the observed ions are expected to be mixtures of isomers, in which the structures shown in Scheme 2 are assumed to prevail. Furthermore, very small amounts of other species like $[VC_2H_7O_2]^+$ are formed, which are not included in Figure 5 and Scheme 2 for the sake of clarity. Another much more abundant V^{IV} species is $[VC_3H_9O_3]^+$ (m/z 144), presumably $V(OCH_3)_3^+$, which seems to evolve as a second terminal product under ICR conditions and is only observed at very long reaction times. As the intensity of $[VC_3H_9O_3]^+$ is not negligibly small, it is accounted for in the above-mentioned modeling by the formation of m/z 144 from m/z 143 (k_9).

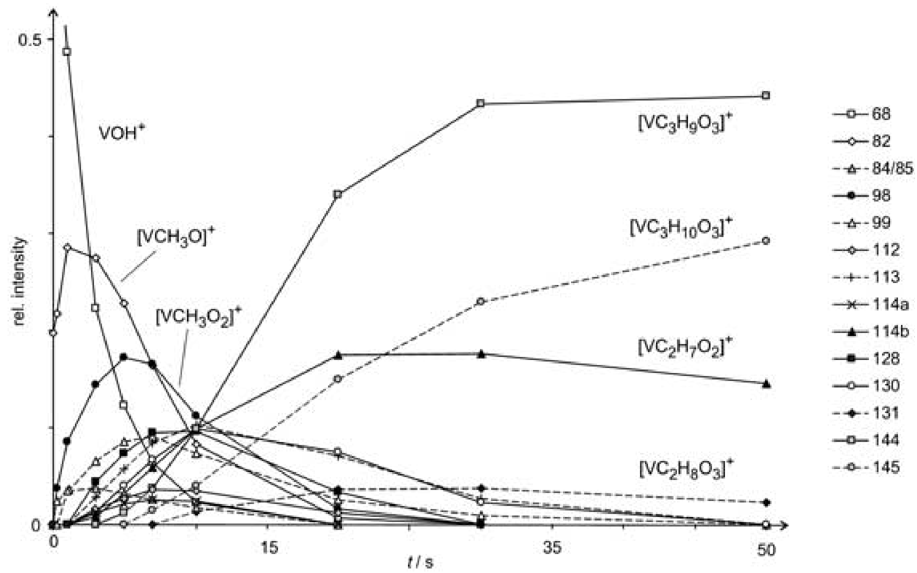

Figure 6. Intensities (normalized to $\Sigma = 100$) for the reaction of methanol with VOH^+. Ions also observed in the methanol/VO^+-system are marked with dashed lines, ions with intensities lower than 1 % at all reaction times are not shown. The legend gives the masses of the observed ions (68: VOH^+, 82: $VOCH_3^+$, 84: VO_2H^+, 85: $VO_2H_2^+$, 98: $[VCH_3O_2]^+$, 99: $[VCH_4O_2]^+$, 112: $[VC_2H_5O_2]^+$, 113: $[VC_2H_6O_2]^+$, 114a: $[VCH_3O_3]^+$, 114b: $[VC_2H_7O_2]^+$, 128: $[VC_2H_5O_3]^+$, 130: $[VC_2H_7O_3]^+$, 131: $[VC_2H_8O_3]^+$, 144: $[VC_3H_9O_3]^+$, 145: $[VC_3H_{10}O_3]^+$). The intensities of the ions VO_2H^+ (m/z 84) and $VO_2H_2^+$ (m/z 85) are so similar throughout the whole reaction time that the two symbols cannot be distinguished; thus, only VO_2H^+ is marked.[61]

The product-ion pattern that evolves in the case of the methanol/VOH^+ system is even more complex than that observed for methanol/VO^+. The condensation product $VOCH_3^+$ (m/z 82) of the very first step reacts with a second methanol molecule to yield $[VCH_3O_2]^+$ (m/z 98), concomitant with the loss of methane. The further reaction cascade comprises at least three subsequent steps and leads to the final product $[VC_3H_9O_3]^+$ (Figure 6). During this process, oxidation from V^{II} to V^{IV} has to occur, because the sequence starts with V^{II} species (VOH^+, $VOCH_3^+$), whereas the final product $V(OCH_3)_3^+$ contains vanadium in the oxidation state +IV. For the intermediates $[VCH_3O_2]^+$ (m/z 98) and $[VC_2H_5O_3]^+$ (m/z 128), both oxidation states are conceivable (Figure 7). Thus, the formation of $[VCH_3O_2]^+$ from methanol and $VOCH_3^+$ can be interpreted as an oxidation to the V^{IV} species $OV(OCH_3)^+$ concomitant with the elimination of methane. The isomeric V^{II} compound $VOH(OCH_2)^+$ might also be present, because the subsequently formed cations $VOCH_3(OCH_2)^+$ (m/z 112) and $VOCH_3(CH_3OH)^+$ (m/z 114) could be regarded as products of this isomer by condensation and ligand exchange with methanol. Particular stability of $[VC_2H_7O_2]^+$ (m/z 114) under the present conditions is implied by the very slow depletion of its intensity (Figure 3). Its further reaction with methanol most probably leads directly to $V(OCH_3)_3^+$ by loss of H_2. The structural ambivalence discussed for $[VCH_3O_2]^+$ also holds

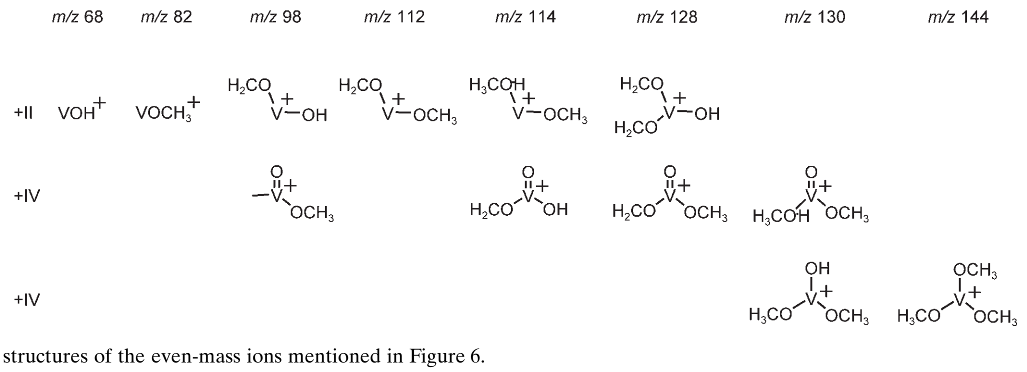

Figure 7. Possible structures of the even-mass ions mentioned in Figure 6.

true for $[VC_2H_5O_3]^+$ (*m*/*z* 128), which formally bears an additional formaldehyde unit. In this case it is even more probable that oxidation to V^{IV} has already occurred because the ion is formed at a later stage of the reaction cascade. Unlike for the main final product $V(OCH_3)_3^+$ (*m*/*z* 144), there are two probable structures with formal V^{IV} for the intermediate $[VC_2H_7O_3]^+$ (*m*/*z* 130): the hydroxide $HOV(OCH_3)_2^+$ and the vanadyl complex $OV(OCH_3)(CH_3OH)^+$. As only condensation to $V(OCH_3)_3^+$ is observed as a further reaction, but no ions with *m*/*z* 159, 160 or 161 (which would be expected as products of the reaction of the vanadyl complex with methanol), the hydroxide structure $HOV(OCH_3)_2^+$ may prevail. Note again that theoretical results indicate a facile isomerization of complexes of this type.[12]

A closer inspection of Figure 6 reveals another important aspect: all reactions discussed so far belong to closed-shell reaction pathways. Yet, the loss of a methyl radical plays a major role in the VOH^+ system as, for example, indicated by the formation of $[VC_2H_8O_3]^+$ from $[VC_2H_7O_2]^+$ and methanol. According to the elemental composition, the V^{III} and V^V species that result from radical loss (broken line in Figure 6) are already known from the methanol/VO^+-cascade (see above).[61] Loss of a methyl radical is not limited to the later steps of the reaction cascade: the formation of $VO_2H_2^+$ from VOH^+ and methanol is already observed in the very first step, albeit only with less than 5% probability.[62] Even though generated by different reaction pathways, the V^{III} and V^V ions in the methanol/VOH^+ system react as described above for the methanol/VO^+ system, resulting in a second parallel reaction cascade finally leading to $V(OCH_3)_2(CH_3OH)^+$. Furthermore, the continuous rise in intensity of $[VC_3H_{10}O_3]^+$, even after a reaction time of 50 s, suggests its direct formation from $V(OCH_3)_3^+$, the final product of the VOH^+ cascade, by abstraction of a hydrogen atom from methanol (Scheme 3).

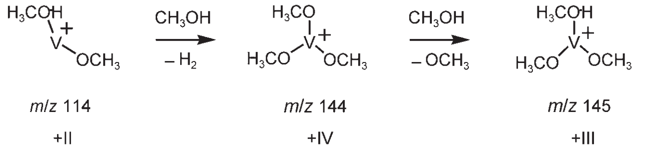

Scheme 3. Reaction sequence in the methanol/VOH^+-system as an example for changes of oxidation state: $V^{II} \rightarrow V^{IV} \rightarrow V^{III}$.

The complete reaction network, starting from VOH^+ and methanol, can therefore be understood as a superposition of two reaction cascades. In addition to ligand-exchange reactions, condensations, and dehydrogenation of methanol to formaldehyde, in all of which the oxidation state of the metal does not change, losses of methane and methyl as well as methoxy radicals are observed. The former induces the oxidation of V^{II} to V^{IV} and gives access to the final product $V(OCH_3)_3^+$. The loss of radicals provide access to V^{III} and V^V species of the methanol/VO^+ cascade, which finally leads to $V(OCH_3)_2(CH_3OH)^+$ (Scheme 3).[63]

In the methanol/VO_2^+ system, the two main products $(CH_2O)VO^+$ and $V(OH)_2^+$ both react with a second methanol molecule to yield $[VCH_4O_2]^+$. This product can therefore be regarded as a mixture of the complex $(CH_3OH)VO^+$ (by ligand exchange of CH_2O for methanol) and the inserted species CH_3OVOH^+ (by condensation of $V(OH)_2^+$ and methanol in analogy to the reaction $VOH^+ \rightarrow VOCH_3^+$ described above). Both ions are intermediates in the methanol/VO^+ reaction cascade and their consecutive reactions have already been discussed for the VO^+ case. The main difference between the VO^+ and the VO_2^+ systems therefore concerns the very first step, mere dehydrogenation versus oxidative dehydrogenation. During the subsequent reactions identical products are nonetheless reached on both pathways. Note that one of the product ions of the reaction cascade is the $VO_2C_2H_6O^+$ species reported by Justes et al. for the reaction of VO_2^+ with methanol.[18]

Several of the ions discussed here show similar behaviour to the fragmentation reactions of $OV(OCH_3)_3^+$, which have previously been studied in detail.[12] At low internal energy, the molecular ion $OV(OCH_3)_3^+$ consecutively loses CH_2O, H_2 or methanol, respectively, so that first V^{IV} and then V^{II} species are formed. Losses of $H^\bullet$ and $CH_3O^\bullet$ are only possible if more energy is available, and provide access to V^V and V^{III} ions. Again, a series of subsequent eliminations of CH_2O, H_2, and CH_3OH take place. This degradation of $OV(OCH_3)_3^+$ (*m*/*z* 160) can be seen as a complementary experiment to the cascade of ion–molecule reactions in the FTICR-MS of this work. The two intermediates with *m*/*z* 97 and 129 are common in both experimental approaches with respect to the methanol–VO^+ system. However, an oxidation to the V^V species $OV(OCH_3)_2(OCH_2)^+$ is not observed in the ion–molecule reactions due to the high oxidation power of V^V species when compared with methanol. During the degradation experiment, which starts with a V^{IV} ion, loss of closed-shell neutral species lead to V^{II} and V^{IV} ions. Such ions are difficult to obtain via VO^+, but readily accessible when starting from VOH^+. Three ions can be found in the fragmentation patterns that are also abundant intermediates in the methanol–VOH^+ system (*m*/*z* 68, 98 and 130). $[VC_3H_9O_4]^+$ (*m*/*z* 160) is not observed as a product of ion–molecule reactions starting from VOH^+ and methanol, even though a change of oxidation state is not necessary when forming this ion from the observed $[VC_2H_7O_3]^+$ (*m*/*z* 130, V^{IV}) and methanol. Obviously, the condensation reaction of a VOH to a $VOCH_3$ group (resulting in $[VC_3H_9O_3]^+$ (*m*/*z* 144) in this case) is again much faster than the dehydrogenation of a methanol molecule (which would lead to $[VC_3H_9O_4]^+$ (*m*/*z* 160)).

Comparison with other metal-oxide ions: It has been shown that the early transition metal oxide ScO^+ reacts with methanol to yield $OSc(OCH_2)^+$, CH_3OScOH^+, and $Sc(OCH_3)_2^+$.[28] Hence, not only the primary product, but also the subsequent products corroborate the analogy to the methanol–VO^+ system. Admittedly, the corresponding products CH_3OYOH^+ and $Y(OCH_3)_2^+$ are generated in the methanol/YO^+ system as well, even though the primary product is $HYOH^+$ instead of $OY(OCH_2)^+$. The reactions of MOH^+ and $MOCH_3^+$ (M = Sc, Y) with methanol were described in the same publication. Like for vanadium, an oxidation to M^{III} species by the elimination of $CH_3^{\bullet}$ or $H^{\bullet}$ is observed in these cases. Similar results have recently been reported for lanthanide cations.[64]

The situation is quite different in the reaction of the late transition-metal-oxide cation FeO^+ with methanol.[29,65] Firstly, the higher selectivity of VO^+ compared with FeO^+ is obvious. For example, the loss of $H^{\bullet}$ is not observed in the reaction of VO^+ with methanol, whereas it is one of the most abundant channels in the case of FeO^+. Secondly, the oxidation of methanol by FeO^+ is an oxidative dehydrogenation, because $Fe(OCH_2)^+$ is formed by loss of H_2O. In contrast, the very strong V–O bond prevents water formation and, in the reaction of VO^+, H_2 is lost instead. This is another example of the effect of the high oxophilicity of the early transition metal vanadium ($D_0(V^+{-}O) = 578 \pm 10\,kJ\,mol^{-1}$)[66] compared with the late transition metal iron ($D_0(Fe^+{-}O) = 341 \pm 6\,kJ\,mol^{-1}$).[67]

Further, MoO^+ has been studied with methanol in an ICR mass spectrometer.[30] It is to be expected that MoO^+ should behave more like VO^+ than FeO^+ because of its proximity in the periodic table. Indeed, the strong Mo–O bond with MoO^+ is also not cleaved upon reaction with methanol. Furthermore, the observed reaction is selective and can also be interpreted as an α oxidation to formaldehyde. Yet, its reactivity is still quite different to that of VO^+: whereas with VO^+ the loss of H_2 is observed, formaldehyde is lost in the reaction of methanol with MoO^+. Like in the above-mentioned transition of $ScO^+ \rightarrow YO^+$, going one row down in the periodic table changes the observed reactivity pattern: the strong M–O bonds which are unlikely to be cleaved for first row elements have to give way to the stronger M–C and M–H bonds possible in the second row.

Conclusion

A comparison of the primary and subsequent ion–molecule reactions of atomic V^+, the hydroxide VOH^+ and the oxides VO^+ and VO_2^+ with methanol reveals that the oxidation state of the metal is a key factor which determines the reactivity of the respective compound. Cations in low oxidation states (i.e., V^+ and VOH^+) reduce methanol, whereas VO_2^+ (V^V) mediates an oxidative dehydrogenation to formaldehyde. VO^+ (V^{III}) also dehydrogenates methanol, but it does not change its oxidation state during this process. The stability of V^{III} under the ion–molecule reaction conditions studied here is further supported by its formation in each major reaction studied in this work, irrespective of the initial oxidation state of the cation. The transitions $+\textsc{i} \rightarrow +\textsc{iii}$ and $+\textsc{v} \rightarrow +\textsc{iii}$ proceed via oxygen-atom transfer, the transitions $+\textsc{ii} \rightarrow +\textsc{iii}$ and $+\textsc{iv} \rightarrow +\textsc{iii}$ via loss of methyl and methoxy radicals, respectively.

Not unexpectedly, simple ligand-exchange reactions ($M(OCH_2)^+ \rightarrow M(CH_3OH)^+$) are faster than the bond activations, which lead to dehydrogenation or oxygen-atom transfer. Yet, condensation reactions ($MOH^+ \rightarrow MOCH_3^+$) are also strongly favored. The process may be seen as a formal ligand exchange of hydroxy and methoxy ligands, but the mechanism must include an additional hydrogen atom transfer. This selectivity for the condensation observed with vanadium hydroxides is worth emphasizing, because condensation reactions are not favored to such an extent with iron or lanthanide hydroxide cations.[64]

The insertion compound CH_3OVOH^+ (**3**) is the most stable species on the potential-energy surface of VO^+/CH_3OH en route to the dehydrogenation of methanol. Its formation can occur via a four-centered transition structure which formally corresponds to an addition of the O–H bond to the vanadyl unit. Elimination of dihydrogen from the insertion intermediate is, however, associated with a considerable barrier, which is located above the energy of the separated reactants. Therefore, this route cannot account for the experimentally observed 1,2-dehydrogenation of methanol mediated by VO^+. Instead, an alternative mechanism for the dehydrogenation of methanol by VO^+ is proposed, which proceeds via an initial C–H bond activation of methanol and involves energy barriers which are consistent with the experimental observations.

Acknowledgements

Financial support by the Deutsche Forschungsgemeinschaft (SFB 546) and the Fonds der Chemischen Industrie is appreciated. We furthermore thank the Konrad-Zuse Zentrum Berlin for generous allocation of computer time.

---

[1] a) *Selective Oxidation by Heterogeneous Catalysis* (Eds.: G. Centi, F. Cavani, F. Trifiró), Kluwer Academic/Plenum Publishers, New York, **2001**; b) J. Hagen, *Technische Katalyse. Eine Einführung*, VCH, Weinheim, **1996**.

[2] *Appl. Catal. A* **1997**, *157* (the entire volume).

[3] a) F. Gilardoni, J. Weber, A. Baiker, *J. Phys. Chem. A* **1997**, *101*, 6069–6076; b) T. V. Andrushkevich, *Catal. Rev. Sci. Eng.* **1993**, *35*, 213–259; c) F. Gilardoni, A. T. Bell, A. Chakraborty, P. Boulet, *J. Phys. Chem. B* **2000**, *104*, 12250–12255; d) K. Chen, E. Iglesia, A. T. Bell, *J. Catal.* **2000**, *192*, 197–203; e) B. Solsona, T. Blasco, J. M. López Nieto, M. L. Peña, F. Rey, A. Vidal-Moya, *J. Catal.* **2001**, *203*, 443–452; f) K. Chen, A. T. Bell, E. Iglesia, *J. Phys. Chem. B* **2000**, *104*, 1292–1299.

[4] a) Y. Zhang-Lin, M. Forissier, R. P. Sneeden, J. C. Védrine, J. C. Volta, *J. Catal.* **1994**, *145*, 256–266; b) Y. Zhang-Lin, M. Forissier, J. C. Védrine, J. C. Volta, *J. Catal.* **1994**, *145*, 267–275.

[5] B. M. Weckhuysen, D. E. Keller, *Catal. Today* **2003**, *78*, 25–46.

[6] C. Limberg, *Angew. Chem.* **2003**, *115*, 6112–6136; *Angew. Chem. Int. Ed.* **2003**, *42*, 5932–5954.

[7] C. Copéret, M. Chabanas, R. Petroff Saint-Arroman, J.-M. Basset, *Angew. Chem.* **2003**, *115*, 164–191; *Angew. Chem. Int. Ed.* **2003**, *42*, 156–181.

[8] a) D. Schröder, H. Schwarz, *Angew. Chem.* **1995**, *107*, 2126–2150; *Angew. Chem. Int. Ed. Engl.* **1995**, *34*, 1973–1995; b) D. K. Böhme, H. Schwarz, *Angew. Chem. 117*, 2388–2254; *Angew. Chem. Int. Ed.* **2005**, *44*, 2336–2354, and references therein.

[9] K. Koszinowski, D. Schröder, H. Schwarz, *Angew. Chem.* **2004**, *116*, 124–127; *Angew. Chem. Int. Ed.* **2004**, *43*, 121–124.

[10] D. Schröder, H. Schwarz, S. Shaik, *Struct. Bonding (Berlin)* **2000**, *97*, 91–123.

[11] Sonderforschungsbereich 546. Structure, dynamics and reactivity of transition-metal oxide aggregates. http://www.chemie.hu-berlin.de/sfb546/index.html

[12] D. Schröder, J. Loos, M. Engeser, H. Schwarz, H.-C. Jankowiak, R. Berger, R. Thissen, O. Dutuit, J. Döbler, J. Sauer, *Inorg. Chem.* **2004**, *43*, 1976–1985.

[13] D. Schröder, M. Engeser, M. Brönstrup, C. Daniel, J. Spandl, H. Hartl, *Int. J. Mass Spectrom.* **2003**, *228*, 743–757.

[14] D. Schröder, M. Engeser, H. Schwarz, E. C. E. Rosenthal, J. Doebler, J. Sauer, unpublished results.

[15] J. N. Harvey, M. Diefenbach, D. Schröder, H. Schwarz, *Int. J. Mass Spectrom.* **1999**, *182*/183, 85–97.

[16] M. Engeser, M. Schlangen, D. Schröder, H. Schwarz, *Organometallics* **2003**, *22*, 3933–3943.

[17] Y. Cao, X. Zhao, B. Xin, S. Xiong, Z. Tang, *J. Mol. Struct.* **2004**, *683*, 141–146.

[18] D. R. Justes, N. A. Moore, A. W. Castleman, Jr., *J. Phys. Chem. B* **2004**, *108*, 3855–3862.

[19] K. Eller, H. Schwarz, *Int. J. Mass Spectrom. Ion Processes* **1989**, *93*, 243–257.

[20] M. Engeser, T. Weiske, D. Schröder, H. Schwarz, *J. Phys. Chem. A* **2003**, *107*, 2855–2859.

[21] G. K. Koyanagi, D. K. Bohme, I. Kretzschmar, D. Schröder, H. Schwarz, *J. Phys. Chem. A* **2001**, *105*, 4259–4271.

[22] D. Schröder, H. Schwarz, D. E. Clemmer, Y.-M. Chen, P. B. Armentrout, V. I. Baranov, D. K. Böhme, *Int. J. Mass Spectrom. Ion Processes* **1997**, *161*, 175–191.

[23] $R = 1.69$ was used for methanol according to: J. E. Bartmess, R. M. Georgiadis, *Vacuum* **1983**, *33*, 149–153.

[24] a) C. Lee, W. Yang, R. G. Parr, *Phys. Rev. B* **1988**, *37*, 785; b) B. Miehlich, A. Savin, H. Stoll, H. Preuss, *Chem. Phys. Lett.* **1989**, *157*, 200; c) A. D. Becke, *J. Chem. Phys.* **1993**, *98*, 5648.

[25] *Gaussian 98*, *Revision A.7*, Gaussian, Inc., Pittsburgh PA (USA), **1998**.

[26] a) P. J. Hay, W. R. Wadt, *J. Chem. Phys.* **1985**, *82*, 270–283; b) P. J. Hay, W. R. Wadt, *J. Chem. Phys.* **1985**, *82*, 284–298; c) P. J. Hay, W. R. Wadt, *J. Chem. Phys.* **1985**, *82*, 299–310.

[27] A. Schäfer, C. Huber, R. Ahlrichs, *J. Chem. Phys.* **1994**, *100*, 5829–5835.

[28] M. Azzaro, S. Breton, M. Decouzon, S. Geribaldi, *Int. J. Mass Spectrom. Ion Processes* **1993**, *128*, 1–20.

[29] D. Schröder, R. Wesendrup, C. A. Schalley, W. Zummack, H. Schwarz, *Helv. Chim. Acta* **1996**, *79*, 123–132.

[30] E. F. Fialko, A. V. Kikhtenko, V. B. Goncharov, *Organometallics* **1998**, *17*, 25–31.

[31] a) T. Su, W. J. Chesnavich, *J. Chem. Phys.* **1982**, *76*, 5183–5185; b) T. Su, *J. Chem. Phys.* **1988**, *88*, 4102–4103; c) T. Su, *J. Chem. Phys.* **1988**, *89*, 5355–5356.

[32] G. Bouchoux, J. Y. Salpin, D. Leblanc, *Int. J. Mass Spectrom. Ion Processes* **1996**, *153*, 37–48.

[33] This limit is further supported by the observation that, among other ions, $VOCH_3^+$ is formed as the major product upon reacting thermalized V^+ with CH_3OCH_3 which implies a lower limit of $D(V^+{-}OCH_3) = 348 \pm 13\,kJ\,mol^{-1}$.

[34] Calculated results for $^4VOCH_3^+$: $d(V{-}O) = 171$ pm, $d(O{-}C) = 143$ ppm, $d(O{-}H) = 109$ pm, $a\ (VOC) = 180°$; $E_0 = -1058.876538$ au. For the reaction $^4VOH^+ + CH_3OH \rightarrow {}^4VOCH_3^+ + H_2O$, this results in $\Delta E_0 = -42\,kJ\,mol^{-1}$, $\Delta E_{298} = -40\,kJ\,mol^{-1}$, $\Delta G_{298} = -41\,kJ\,mol^{-1}$.

[35] For a similar methanolysis of $FeOH^+$, also see: A. Fiedler, D. Schröder, H. Schwarz, B. L. Tjelta, P. B. Armentrout, *J. Am. Chem. Soc.* **1996**, *118*, 5047–5055.

[36] M. R. Sievers, P. B. Armentrout, *J. Chem. Phys.* **1995**, *102*, 754–762.

[37] R. C. Bell, K. A. Zemski, D. R. Justes, A. W. Castleman, Jr., *J. Chem. Phys.* **2001**, *114*, 798–811.

[38] M. Calatayud, B. Silvi, J. Andrés, A. Beltrán, *Chem. Phys. Lett.* **2001**, *333*, 493–503.

[39] a) D. Schröder, S. Shaik, H. Schwarz, *Acc. Chem. Res.* **2000**, *33*, 139–145; b) H. Schwarz, *Int. J. Mass Spectrom.* **2004**, *237*, 75–105, and references therein.

[40] L. Gracia, J. Andrés, V. S. Safont, A. Beltrán, *Organometallics* **2004**, *23*, 730–739.

[41] D. K. Bohme, *Int. J. Mass Spectrom. Ion Processes* **1992**, *115*, 95–110.

[42] T. C. Jackson, T. J. Carlin, B. S. Freiser, *J. Am. Chem. Soc.* **1986**, *108*, 1120–1126.

[43] R. C. Burnier, G. D. Byrd, T. J. Carlin, M. B. Wiese, R. B. Cody, B. S. Freiser, *Lect. Notes Chem.* **1982**, *31*, 98–118.

[44] N. N. Greenwood, A. Earnshaw, *Chemistry of the Elements*, Pergamon, Oxford, **1984**, p. 1142.

[45] W. L. Hase, W. Koch, *Int. J. Mass Spectrom.* **2000**, *201*, ix–x (Foreword); the whole issue deals with theoretical/computational studies of ionic systems and the impact of computational chemistry of the structures, energetics, and kinetics of gas-phase ions.

[46] M. C. Holthausen, in *The Encyclopedia of Mass Spectrometry*, *Vol. 1* (Ed.: P. B. Armentrout), Elsevier, **2005**, p. 77–89.

[47] a) H. Schwarz, D. Schröder, *Pure Appl. Chem.* **2000**, *72*, 2319–2332; b) N. Fröhlich, G. Frenking, in *Quantum-Mechanical Prediction of Thermochemical Data* (Ed.: J. Cioslowski), Kluwer, Dordrecht, **2001**, p. 199–233; c) H. Schwarz, *Angew. Chem.* **2003**, *115*, 4580–4593; *Angew. Chem. Int. Ed.* **2003**, *42*, 4442–4454; d) J. M. Mercero, J. M. Matxain, X. Lopez, D. M. York, A. Largo, L. A. Erikson, J. M. Ugalde, *Int. J. Mass Spectrom.* **2005**, *240*, 37–99.

[48] P. E. M. Siegbahn, R. H. Crabtree, *Struct. Bonding (Berlin)* **2000**, *97*, 125–144.

[49] Y. Shiota, K. Yoshizawa, *J. Am. Chem. Soc.* **2000**, *122*, 12317–12326.

[50] L. Gracia, J. R. Sambrano, V. S. Safont, M. Calatayud, A. Beltrán, J. Andrés, *J. Phys. Chem. A* **2003**, *107*, 3107–3120.

[51] W. Koch, M. C. Holthausen, *A Chemist's Guide to Density Functional Theory*, Wiley-VCH, Weinheim, **2000**.

[52] D. Schröder, M. Engeser, H. Schwarz, J. N. Harvey, *ChemPhysChem* **2002**, *3*, 584–591.

[53] M. Pykavy, C. van Wüllen, *J. Phys. Chem. A* **2003**, *107*, 5566–5572.

[54] The corresponding bond dissociation energies are $D_0(H_3CO{-}H) = 437\,kJ\,mol^{-1}$, $D_0(HOCH_2{-}H) = 411\,kJ\,mol^{-1}$, and $D_0(H_3C{-}OH) = 386\,kJ\,mol^{-1}$ (taken from ref. [59]).

[55] According to pre-optimization results, $OVOH(CH_3)^+$, as a potential intermediate of case iii-a), is about $100\,kJ\,mol^{-1}$ more stable than the isomeric hydride complex $HVO(OCH_3)^+$ (singlet surface, the triplet surface lies about $80\,kJ\,mol^{-1}$ higher). Pathway iii-b) leads to the intermediate $HOVOCH_3^+$ of path i-b). As discussed there, this intermediate is a dead end for methanol dehydrogenation without any viable way to the experimentally observed exit channel.

[56] This has been verified by intrinsic reaction coordinate (IRC) calculations for the triplet surface.

[57] For triplet **TS4/5**, $\langle S^2 \rangle = 2.5$ has been calculated, suggesting the need to check this structure by more accurate theoretical methods. On the singlet surface, **TS4/5** did not converge when using the TZVP basis set; it is situated $71\,kJ\,mol^{-1}$ above the triplet species at the B3LYP/Lanl2DZ-level.

[58] J. W. Gauld, L. Radom, *J. Am. Chem. Soc.* **1997**, *119*, 9831–9839.

[59] NIST Standard Reference Database: http://webbook.nist.gov/chemistry/

[60] Note that mere association reactions are disfavored under the low-pressure ICR conditions, but the probability rises with increasing size of the system.

[61] Due to low abundances (<5%), ions with m/z 129 and 143 are not included in Figure 6 for the sake of clarity.

[62] The process $VOH^+ + CH_3OH \rightarrow V(OH)_2^+ + CH_3^{\bullet}$ is estimated to be exothermic by $-50\,kJ\,mol^{-1}$ (refs. [21] and [40]).

[63] Note that the loss of a methyl radical causes an oxidation of formal V^{II} to V^{III}, whereas expulsion of a methoxy radical is associated with a reduction from V^{IV} to V^{III}.

[64] J. M. Carretas, J. Marçalo, A. Pires de Matos, *Int. J. Mass Spectrom.* **2004**, *234*, 51–61.
[65] See also: M. Heninger, P. Pernot, H. Mestdagh, P. Boissel, J. Lemaire, R. Marx, G. Mauclaire, *Int. J. Mass Spectrom.* **2000**, *199*, 267–285.
[66] D. E. Clemmer, N. Aristov, P. B. Armentrout, *J. Phys. Chem.* **1993**, *97*, 544–552.
[67] S. K. Loh, E. R. Fisher, L. Lian, R. H. Schultz, P. B. Armentrout, *J. Phys. Chem.* **1989**, *93*, 3159–3167.
[68] M. W. Chase, Jr., *J. Phys. Chem. Ref. Data* **1998**, *9*, 1–1951.
[69] J. Berkowitz, G. B. Ellison, D. Gutman, *J. Phys. Chem.* **1994**, *98*, 2744–2765.

Received: December 30, 2004
Revised: May 8, 2005